Jeomorfolojik Araştırmalar Dergisi
Journal of Geomorphological Researches
© Jeomorfoloji Derneği www.dergipark.gov.tr/jader E - ISSN: 2667 - 4238

Araştırma Makalesi / Research Article

The Impact of DSM Resolution and Block Geometry on 3D Rockfall Modeling: The Case of Başköy Heritage Site

SYM Çözünürlüğü ve Blok Geometrisinin 3B Kaya Düşmesi Modellemesine Etkisi: Başköy Miras Alanı Örneği

Mustafa UTLU[a], Mehmet Fatih AKGÜMÜŞ[b], Mutluhan AKIN[c]

[a] Sorumlu Yazar / Corresponding Author
Marmara Üniversitesi, İnsan ve Toplum Bilimleri Fakültesi, Coğrafya Bölümü, İstanbul, TÜRKİYE
utlumus@gmail.com https://orcid.org/0000-0002-7508-4478
[b] Milli Eğitim Bakanlığı, Niğde, TÜRKİYE
fatihsungur510@gmail.com https://orcid.org/0000-0002-6844-8712
[c] Nevşehir Hacı Bektaş Veli Üniversitesi, Mühendislik ve Mimarlık Fakültesi, Jeoloji Mühendisliği Bölümü, Nevşehir, TÜRKİYE
mutluhanakin@nevsehir.edu.tr https://orcid.org/0000-0002-5752-6949

Makale Tarihçesi
Geliş 20 Mayıs 2026
Kabul 25 Haziran 2026

Article History
Received: 20 May 2026
Accepted: 25 June 2026

Keywords
3D Rockfall modeling, UAV-DSM, Different resolutions, Block geometry, Rockfalls

Anahtar Kelimeler
3B Kaya Düşmesi Modellemesi, İHA-SYM, Farklı Çözünürlükler, Blok Geometrisi, Kaya Düşmeleri

Atıf Bilgisi / Citation Info
Utlu, M., Akgümüş, M. F. & Akın, M. (2026) The Impact of DSM Resolution and Block Geometry on 3D Rockfall Modeling: The Case of Başköy Heritage Site, Jeomorfolojik Araştırmalar Dergisi / Journal of Geomorphological Researches, 2026 (17): 4

doi: 10.46453/jader.1955333

ABSTRACT

This study evaluates the impact of using UAV-derived DSM data at different resolutions and with different rock block geometries on 3D rockfall modeling, a widely used approach in rockfall simulations. The study area, the Başköy settlement, is an active, rockfall-prone region and has been officially declared a disaster area due to ongoing rockfall events. The main objective of this study is to understand the effects of UAV-derived DSM data with resolutions of 25 cm, 50 cm, and 1 m, together with the use of rock blocks of different geometries, on 3D rockfall simulations. EOTA, Equant, and Elongated rock blocks were used in the study, and the volumetric and weight characteristics of these rock blocks were numerically similar to each other to some extent. A total of 9 rockfall models were carried out using the RAMMS::Rockfall software. During the modeling process, 100 rock blocks were simulated from each source zone, for a total of 20,000 rock blocks. As outputs of the modeling, kinetic energy (kJ), velocity (m/s), jump height (m), and number of deposited rocks were obtained. Accordingly, the highest velocity and kinetic energy values were obtained using the 25 cm resolution DSM data, whereas the highest jump height value was only observed for the Equant rock block in the 50 cm DSM dataset. The lowest values were obtained from the 1 m DSM dataset because of its smoother, less detailed topographic representation. Using 4,299 fallen rock blocks identified from the orthomosaic data, the relationships among different number of deposited rocks datasets, heat maps, and modeled rock blocks were validated using distance-based analysis. Based on these analyses, the 50 cm DSM resolution and the Elongated block type produced the most accurate results.

ÖZET

Bu çalışma, kaya düşmesi simülasyonlarında yaygın olarak kullanılan 3 boyutlu (3D) kaya düşmesi modellemesi üzerinde, İHA (İnsansız Hava Aracı) temelli farklı çözünürlükteki Sayısal Yüzey Modeli (SYM) verilerinin ve farklı kaya bloğu geometrilerinin etkilerini değerlendirmektedir. Çalışma alanı olan Başköy yerleşimi, aktif bir kaya düşmesi bölgesi olup, süregelen kaya düşmesi olayları nedeniyle resmî olarak 'Afete Maruz Bölge' ilan edilmiştir. Çalışmanın temel amacı; 25 cm, 50 cm ve 1 m çözünürlükteki İHA temelli SYM verilerinin, farklı kaya bloğu geometrileriyle birlikte 3D kaya düşmesi simülasyonları üzerindeki tekil ve birleşik etkilerini anlamaktır. Modelleme kapsamında test bloğu (EOTA), Equant (Eşkenar boyutlu) ve Elongated (Uzunlamasına) kaya bloğu geometrileri kullanılmış; bu blokların hacimsel ve ağırlık karakteristikleri sayısal olarak birbirine yakın tutulmuştur. RAMMS::Rockfall yazılımı kullanılarak toplam 9 farklı kaya düşmesi senaryosu modellenmiştir. Modelleme kapsamında, her bir kaynak alandan 100 kaya bloğu bırakılmış ve toplamda 20.000 kaya bloğu simüle edilmiştir. Modelleme sonucunda temel kinematik parametreler olan kinetik enerji (kJ), hız (m/s), sıçrama yüksekliği (m) ve duran (depolanan) kaya bloklarının mekânsal dağılımı elde edilmiştir. Elde edilen bulgulara göre, en yüksek hız ve kinetik enerji değerlerine 25 cm çözünürlüklü SYM verisiyle ulaşılırken, en yüksek sıçrama yüksekliği yalnızca 50 cm çözünürlüklü SYM veri setindeki 'Equant' kaya bloğunda gözlenmiştir. Topografyayı daha pürüzsüz ve daha az detaylı yansıtması nedeniyle en düşük değerler, 1 m çözünürlüklü SYM veri setinde ortaya çıkmıştır. Ortomozaik verileri üzerinden haritalanan 4.299 gerçek kaya bloğu referans alınarak, farklı modelleme sonuçlarına ait depolanan kaya bloklarının sayısı ve modellenen kaya blokları arasındaki ilişkiler mesafe tabanlı analizlerle doğrulanmıştır. Yapılan doğrulama analizleri sonucunda, saha verileriyle en uyumlu ve en doğru sonuçların 50 cm SYM çözünürlüğü ile 'Elongated' blok tipinde elde edildiği belirlenmiştir.

1. INTRODUCTION

Rockfalls are among the most dangerous types of mass movements and natural hazards, frequently occurring instantly under various conditions in many regions of the world, especially along steep, high-gradient slopes (Guzzetti et al., 2004; Alvioli et al., 2021; Alvioli et al., 2023). Rockfall events also observed in high, rugged terrain and along cliffed coastlines are occurring with increasing frequency (Sarkar et al., 2024). They impose significant pressure on infrastructure, environment, and transportation corridors, causing serious problems that can even reach catastrophic levels, resulting in loss of life (Alvioli et al., 2021; Milan et al., 2023). Rockfall events can be influenced by a wide range of factors; such as freeze–thaw processes, day–night temperature differences, and changes in the frequency and intensity of precipitation have intensified with global climate change and, together with anthropogenic factors, have led to more frequent rockfall events (Volkwein et al., 2011; Hungr et al., 2014). Therefore, understanding the hazard and risk potential associated with rockfall events is critical for implementing necessary preventive measures (Milan et al., 2023; Lanfranconi et al., 2023; Massaro et al., 2024). In this context, identifying the hazard and risk dynamics or potentials of rockfalls involves a multi-stage process, including the determination of block geometries, stability conditions, and source zones, as well as the identification of failure mechanisms of the slopes generating these events (Corominas et al., 2014; Mavrouli et al., 2015; Kakavas & Nikolakopoulos, 2022).

Considering the geological and topographic characteristics of the terrain where rock blocks are located, as well as their geometry and volume (Ulamış, 2026), a rock block that detaches rapidly under gravity undergoes a combination of free fall, bouncing, rolling, and sliding (Varnes, 1978). To better understand this behavior, many software have been used for rockfall modeling at different spatial scales, which are widely used and generally conducted using 2D (two-dimensional) and 3D (three-dimensional) approaches (Loye et al., 2009; Žabota et al., 2019). 2D models typically simulate the motion of a single rock block along predefined profiles and are limited to cross-sectional analyses. Thus, they are unable to represent the spatial distribution of rockfall trajectories across the entire study area (Ulamış, 2026). For this reason, 3D rockfall models have been preferred due to the high surface roughness in complex topographies (Crosta et al., 2015; Vagionakis et al., 2026). 3D rockfall modeling provides significant advantages for better understanding these patterns and for effectively evaluating the uncertain conditions generated by falling rock blocks (Lan et al., 2010; Akın et al., 2021). This is because outputs from 3D modeling, such as the number of simulations, rock block types, rockfall source line determination, and resulting kinetic energy, velocity, and jump heights, are highly valuable for hazard and risk assessment and geomorphological studies (Utlu et al., 2020b; Sarro et al., 2025). Moreover, these models provide critical insights into the attenuation behavior, trajectories, and spreading patterns of falling blocks, which constitute essential inputs for such (Carlà et al., 2019; Gallo et al., 2021; Sarkar et al., 2024).

Although 3D modeling provides powerful tools, interpreting model outputs can be problematic when input data are not precisely defined (Crosta et al., 2015). Therefore, in rockfall modeling, data acquired from platforms such as UAVs, LiDAR, and TLS, with centimeter-level accuracy and resolution, provide significant advantages in complex terrains (Utlu et al., 2020a; Vagionakis et al., 2026). Because it is so important to understand rock block behavior. Especially, their trajectories, attenuation characteristics, and deposition zones (Crosta et al., 2015). Thus, detailed surface data, essential base layers in rockfall modeling, are for designing appropriate mitigation measures and preventive engineering structures (Abellan et al., 2006; Jaboyedoff et al., 2012; Chatziangelis et al., 2025). Furthermore, such highly detailed and high-resolution topographic data are also important for accurately representing existing surface features, both because these elements may act as natural barriers influencing the current frictional conditions and because they contribute to the accurate implementation of the modeling process (Crosta et al., 2015).

Despite all these critical processes and the widespread application of 3D modeling based on high-resolution DSM data today, the question of what centimeter- or meter-level resolution should be used still remains unanswered. In addition, another important issue that requires clarification concerns the purpose for which different rock block types should be preferred and utilized during the modeling process. In this context, several studies in the international literature have addressed this issue. (Bartelt et al., 2016; Bühler et al., 2016; Žabota et al., 2019; Caviezel et al., 2021; Kakavas et al., 2022; Ringenbach et al., 2023; Utlu & Şimşek, 2025; Arsenith, 2025; Zengin & Ulamış, 2025).

This study aims to investigate the effects of DSM data at different resolutions and rock block types on rockfall modeling and to reveal the complex nature and behavioral characteristics of rockfall events using Rapid Mass Movement (RAMMS:: Rockfall) software. Within this scope, UAV-derived DSM datasets with resolutions of 25 cm, 50 cm, and 1 m, together with EOTA, Equant, and elongated rock-block geometries, were used. Furthermore, this study differs from many previous studies by using three high-resolution UAV-DSM datasets and three rock block geometries. In addition, the results were validated for accuracy using rock blocks observed in the field. In addition, based on the obtained results, an attempt was made to determine the most suitable resolution and block geometry for modeling complex topographies.

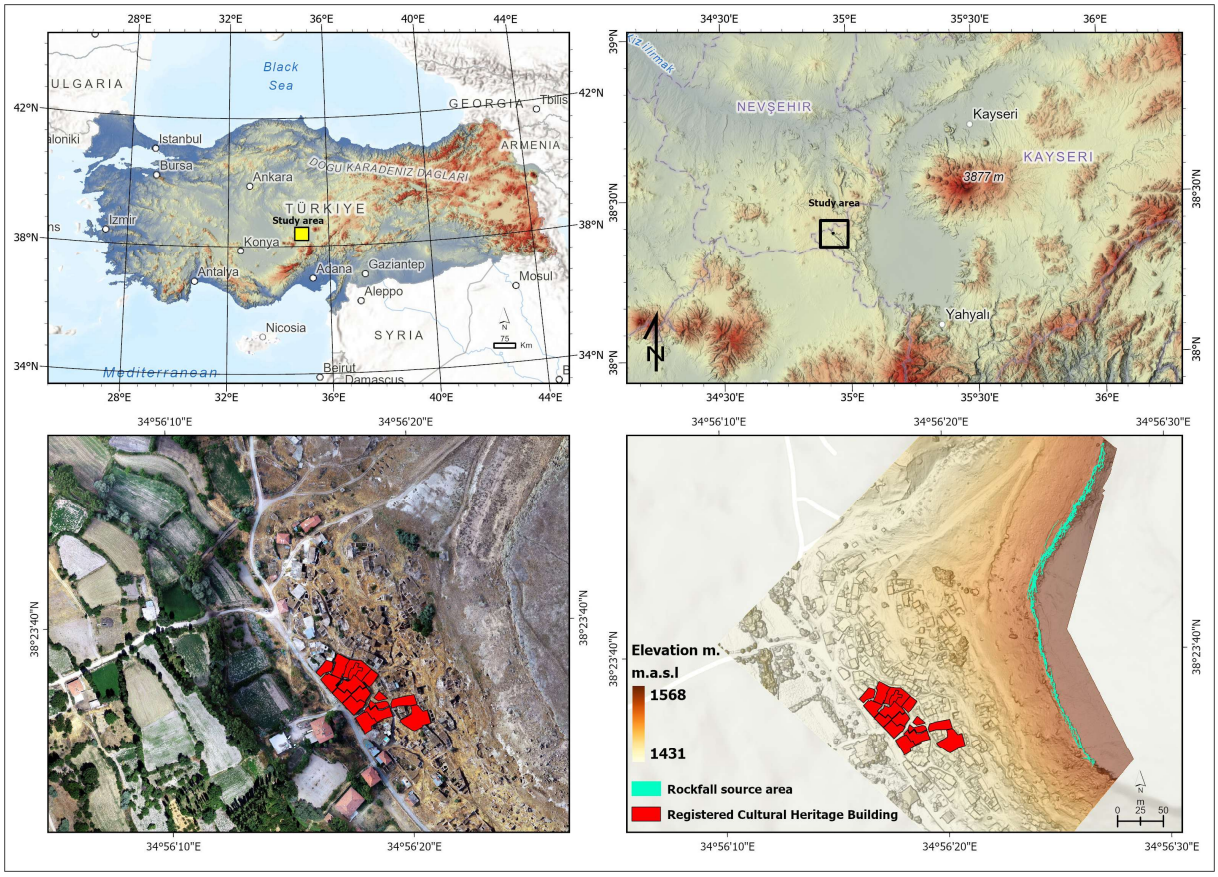

Figure 1: The location of the study area.

2. METHODOLOGY

2.1. Study Area

The study area is located in the Soğanlı Valley, within the Başköy Neighborhood of the Yeşilhisar district in Kayseri, situated in the Central Anatolia Region of Türkiye (Figure 1). The study area, located along the Yeşilhisar–Derinkuyu road, is bordered by Yeşilhisar to the east, Derinkuyu to the west, Ürgüp to the north, and Niğde to the south (Figure 1). The region has been exposed to rockfall events up to the present day. As a result of these events, 13 houses were destroyed in 1963, 31 in 1993, 11 in 2008, and 57 in 2013 (AFAD, 2021). Due to these incidents, the Başköy settlement was declared a disaster area in 2011 by the Disaster

and Emergency Management Presidency (AFAD). Despite being designated as a disaster-prone area, habitation still continues within and around the study area today. Within the boundaries of the Başköy settlement, the Saint George Church, dating back to the 13th century, as well as rock-carved structures and former Greek settlements, are under protection status due to their cultural heritage significance (Figure 1), and these structures are being damaged by rockfall events (Figure 2(a)–(e)). Therefore, evaluating and assessing the rockfall potential of the area is of great importance.

Lithologically, the area is composed of Late Miocene ignimbrite units (Erol, 1983). These ignimbrites represent the earliest products of the volcanism that began in the Upper Miocene in Mount Erciyes. The tuff–ignimbrite sequence is the most widespread unit formed during the initial volcanic phase (Sür, 1972; Figure 3(a)). The tuffs and ignimbrites in the area are locally deeply incised. As a result of the dissection of ignimbrite plateaus, cornices and steep slopes are observed, especially in areas where resistant ignimbrites occur at the upper levels (Somuncu, 1988; Pasquare, 1988). The overall stratigraphy has very steep slopes (90°; Figure 3(b)). The presence of slope gradients up to 90° and the structural weakness of ignimbrites result in inevitable, ongoing rockfall. Thus, the study area represents an important case site in Başköy for understanding both the effects of high-resolution DSM data and the influence of different block geometries. Between the ignimbrite levels, lacustrine deposits are also present. These deposits can reach several meters in thickness, further increasing the instability of the Kızılkaya ignimbrite and contributing to rockfall events. The underlying unit is the Cemilköy ignimbrite. Between the ignimbrite layers, volcanosedimentary units are also present, including fallen blocks and slope-debris deposits (Figure 3(a)-(b)).

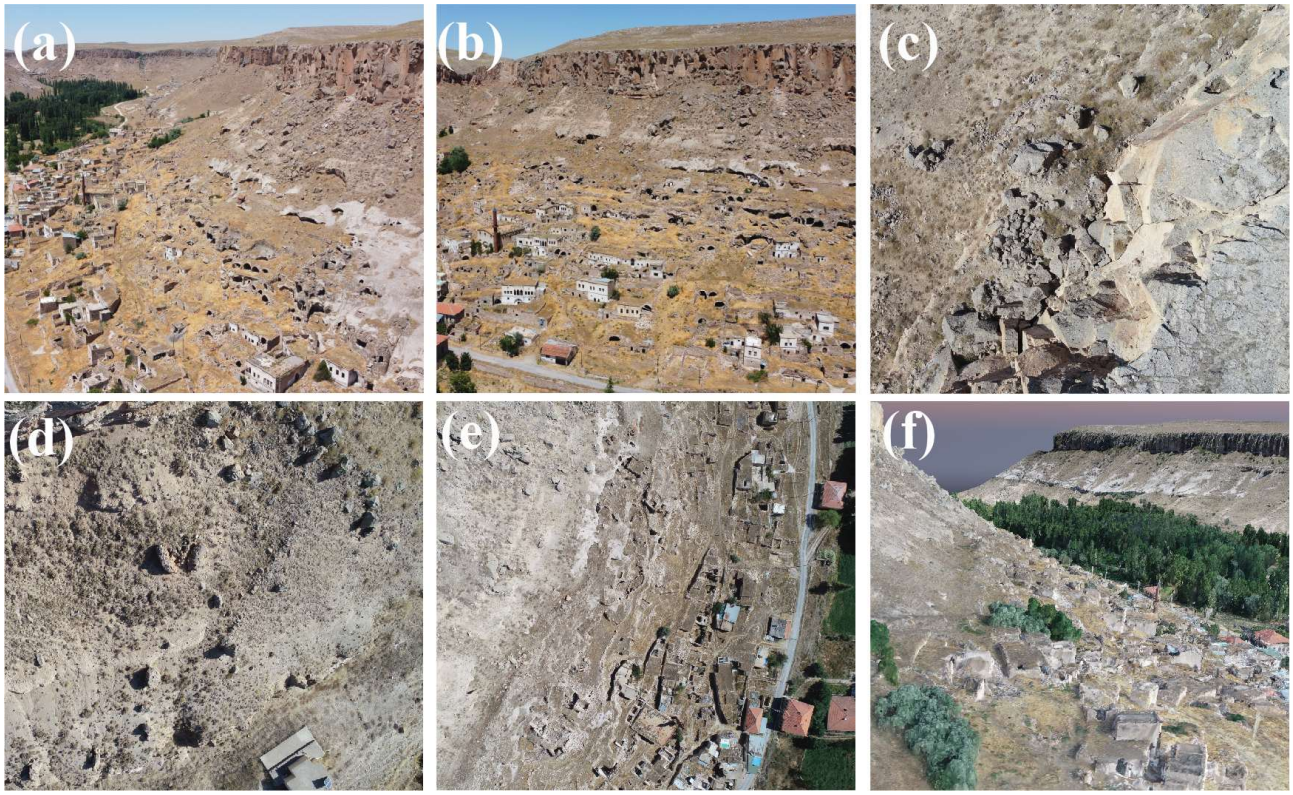

Figure 2: (a)–(b) The Başköy settlement, a 1st-degree protected archaeological site located on steep slopes and exposed to significant rockfall hazard and risk; (c)–(d) Rock blocks detached from ignimbrites with slope angles up to 90° and thicknesses of 10–15 m., (f) Dense point cloud and textured mesh representation of the study area.

2.2. Preparation of spatial database for 3D Rockfall Modeling

The workflow developed to evaluate the effects of different DSM resolutions and rock block geometries within the scope of 3D rockfall modeling is presented in Figure 4.

Field survey and identification of source areas: Field investigations were conducted to

identify active rockfall source zones. During these surveys, detailed observations of fallen rock blocks were conducted, including their geometric characteristics and lithological properties. Based on these observations, potential source areas and representative block characteristics were defined for modeling.

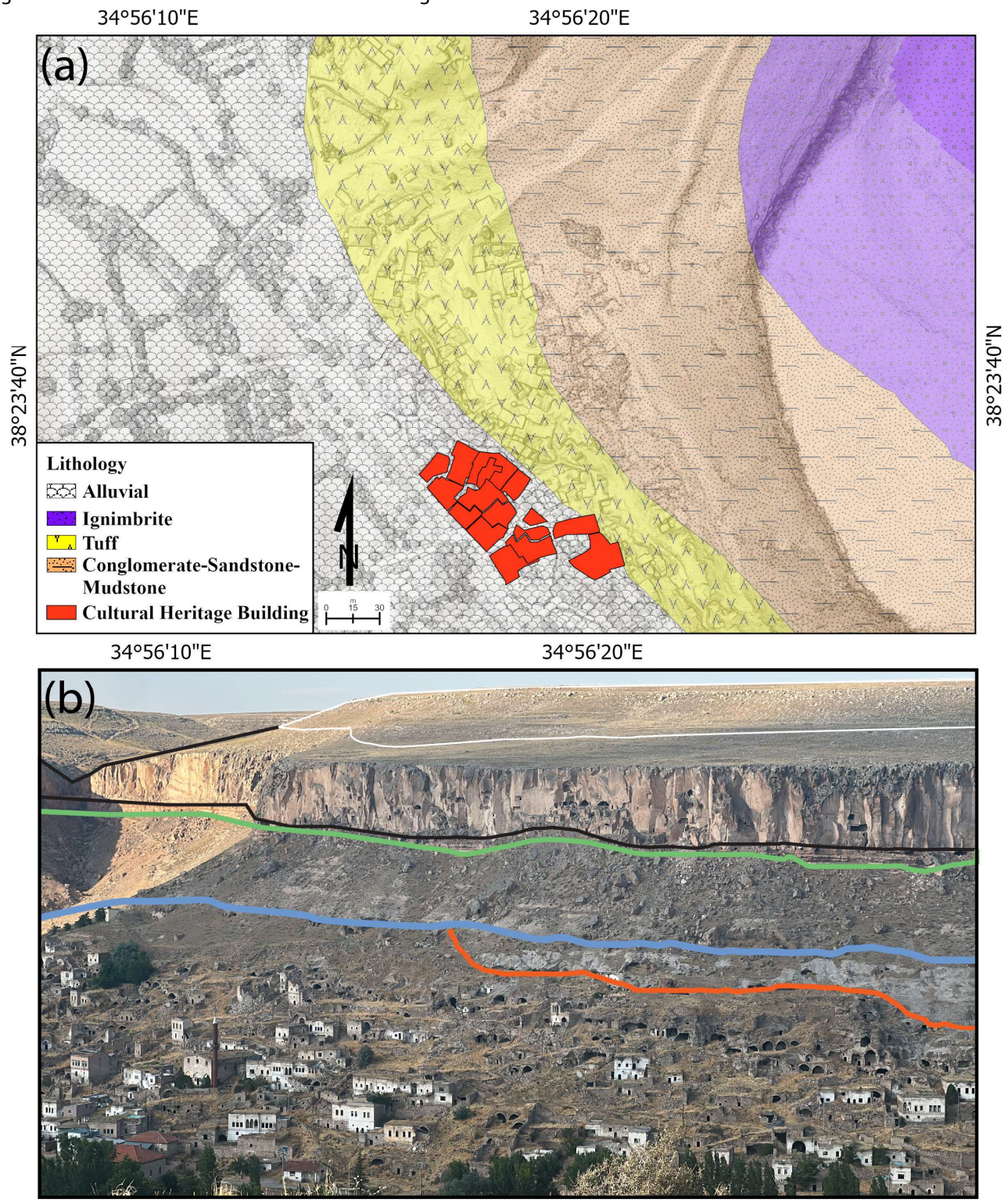

Figure 3: (a) General lithology of the study area (adapted from Atabey, 1989; modified from the 1:100,000 scale MTA Geological Map Series, L33 Sheet), (b) Oblique stratigraphic view obtained from UAV image; white line Kışladağ limestone, black line is Kızılkaya ignimbrite, and source area zone, green line is lacustrine sediments, blue line is volcanosedimantary line, and red line is Cemilköy ignimbrite.

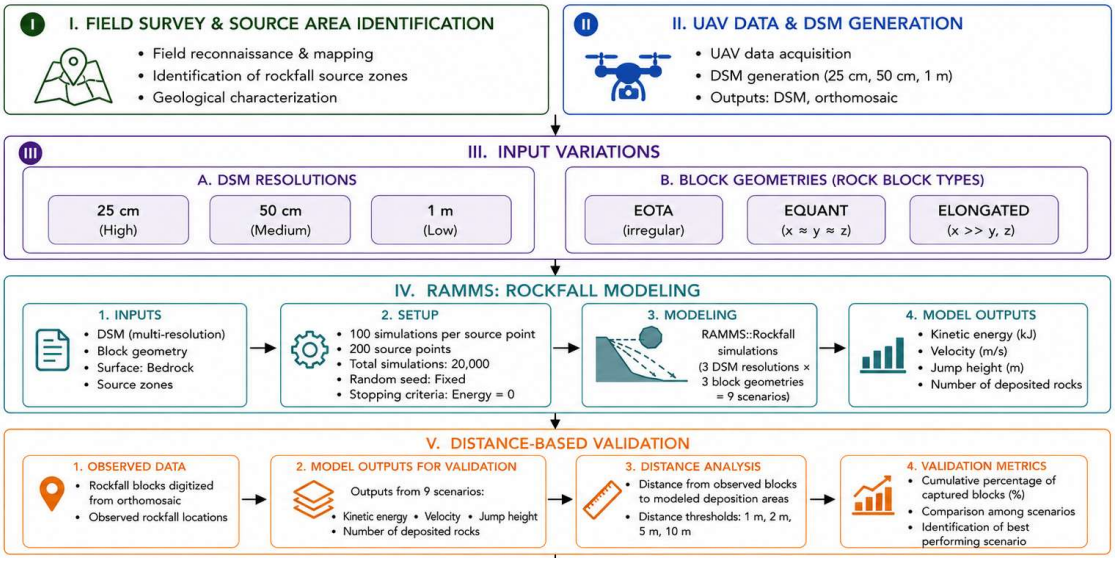

Figure 4. The general flowchart of the rockfall modeling.

Determination of block size and geometric characteristics: Based on field observations, the use of rock blocks with realistic geometries is critical for rockfall modeling (Öztürk et al., 2022). For this purpose, large-volume blocks (elongated) were selected based on field observations of fallen rock blocks. Also, two different rock blocks were selected from the RAMMS: Rockfalls Library, together with an elongated block, to get a different scenario. Thus, the use of large-volume blocks in the modeling process enabled the determination of maximum possible values, such as velocity and kinetic energy.

UAV-DSM generation: A DJI Phantom Pro+ device was used to produce high-resolution DSM and orthomosaic datasets. Prior to the flights, ground control points (GCPs) were established. Within a 20 ha area, 420 stereo images were collected at an altitude of 100 m with a 70% overlap ratio. The trial version of Pix4Dmapper was used to generate the DSM and orthomosaic datasets. The horizontal accuracy of the DSM (RMSE_XY) was ±2.5 cm, while the vertical accuracy (RMSE_Z) was ±3.8 cm.

Rockfall modeling: RAMMS:: ROCKFALL 2.0.10 software was used to model 3D DSMs and 3 block types. In this context, DSM data and terrain properties (bedrock) were used as input datasets.

Modeling outputs: As a result of simulations with three different rock block types, outputs included kinetic energy (kJ), jump height (h), velocity (m/s), and the number of deposited rocks.

2.3. 3D Rockfall Simulations using RAMMS: Rockfall

The RAMMS: Rockfalls is one of the 3D rockfall software which widely preferred hazard and risk assessment hilly and mountainous region in the world (Schraml et al., 2015; Wendeler et al., 2017; Caviezel et al., 2019; Bolliger et al., 2024; Jacobs et al., 2026). In this study, RAMMS, rockfall software, was also used to create 3D models of rock blocks at different resolutions, DSM data, and block types in the study area. The RAMMS: Rockfalls software performs simulations by considering both the translational and rotational motions of falling rock blocks. The algorithm used in the modeling process is rigid-body dynamics. This algorithm accounts for the conversion of kinetic energy into rotational energy during the interaction between the falling rock block and the ground surface (Christen et al., 2014; Vo, 2015). The RAMMS Rockfall program requires several input datasets and parameters to perform rockfall simulations. These include: (i) ground surface properties, which play a critical role in controlling rock block movement and energy dissipation during rockfall events; (ii) the geometry and numerical characteristics of rock blocks; (iii) forest cover, which can act as an effective natural barrier by rapidly dissipating the energy of falling rock blocks. Therefore, the presence or absence of forest cover within the modeling area must be identified; (iv) a Digital

Surface Model (DSM); (v) source zone lines representing potential rockfall initiation areas; and (vi) the number of simulations assigned to the source zones. Within the scope of this study, the rockfall modeling was performed using bedrock surface properties, rock block geometries (EOTA, Equant, and Elongated), forest cover (open forest with sparse density), DSM datasets with spatial resolutions of 25 cm, 50 cm, and 1 m, and source zones. These datasets were derived from high-resolution orthomosaic imagery and incorporated into the modeling process. Within this framework, UAV-derived DSMs at resolutions of 25 cm, 50 cm, and 1 m were used (Figure 5), while the rock block types employed in the simulations are shown in Figure 5 and Table 1. The Kızıldağ ignimbrite formation represents the lines that serve as sources of rockfall events. The identification of the source zones was carried out through field investigations and, more extensively, through orthomosaic imagery, as the source zones were clearly identifiable. These lines correspond to very steep slopes with inclinations reaching up to 90°. A total of 200 source points were automatically generated within the polygon-defined source zones, and 100 rock blocks were released from each point. Thus, the maximum trajectory distributions of a total of 20,000 rock blocks were investigated. In this way, 3D modeling was performed using DSM datasets at three different resolutions, and rock blocks with three different geometries, but with similar weight and volume characteristics. Within this context, the behavior of different rock block types under varying resolutions was evaluated. Particular attention was given to assessing the influence of high-resolution DSM data on rockfall modeling in highly complex topography. This is because high-resolution datasets possess very detailed and rough surface characteristics, which have a critical impact on rockfall behavior. Therefore, the study not only evaluated scenarios involving DSM datasets at different resolutions but also included scenarios modeling different rock block types. The rock blocks considered in the analyses weighed approximately 10.6–13.5 tons, had volumes of 3.94–5.03 m³, and had a density of 2700 kg/m³ (Table 1).

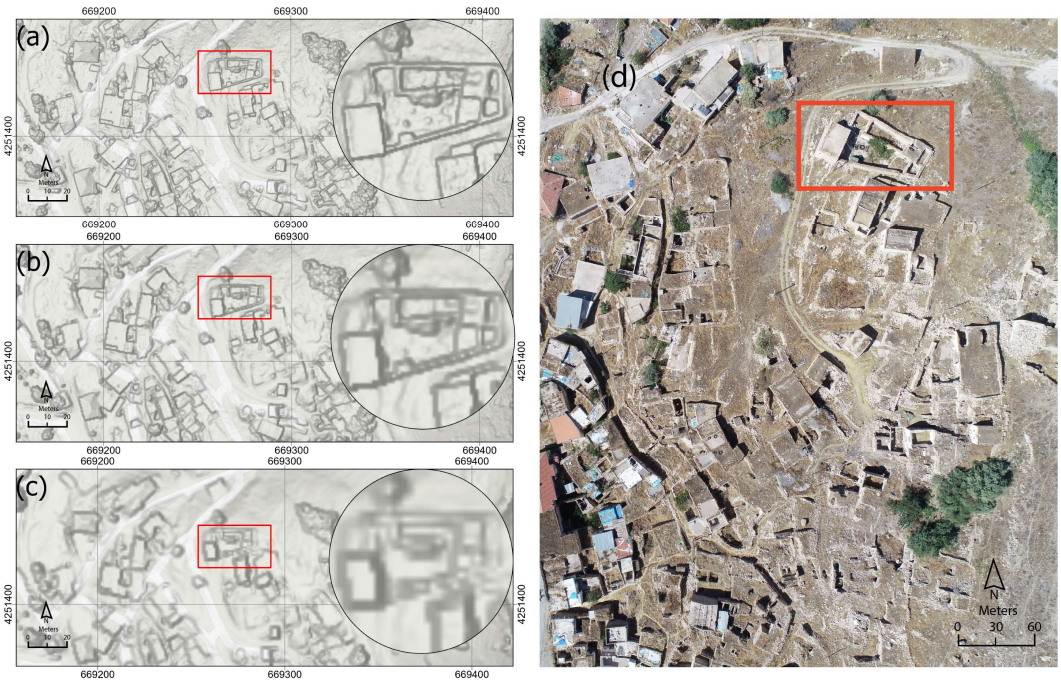

Figure 5: Different resolution UAV-DSM (a) 25 cm, (b) 50 cm, and (c) 1 m; (d) and sample area.

2.4. Rock Blocks Used in the Modeling

In 3D rockfall modeling, the selection of rock block geometry directly affects the modeling results. In particular, not only the geometry of the rock blocks but also their volume and weight characteristics are of great importance. These properties influence the behavior of the rock blocks during their fall and may either facilitate the understanding of their

propagation and attenuation trajectories or make them even more complex. Therefore, the selection of appropriate rock blocks is essential for obtaining reliable results (Dorren and Kühne, 2016; Mary Vick et al., 2019; Torsello et al., 2021; Utlu et al., 2021; Utlu et al., 2023). In this study, three different block types were included in the modeling process. These block types are (a) EOTA, (b) Equant, and (c) Elongated (Figure 6). Considering three different block types was preferred to eliminate modeling limitations that could arise from using a single block geometry. The elongated block type was selected by considering the geometric characteristics of falling blocks (Figure 7). This block type was chosen to obtain more realistic, accurate modeling results and represents the blocks formed by rockfall events on the ignimbrites in the study area. The attribute information of the blocks used in the simulations is presented in Table 1.

a) EOTA: It has more chamfered corners and a more circular concrete-block geometry, and it is commonly used for testing barrier performance. Due to its structural characteristics, this rock block can easily overcome surface roughness. (Ringenbach et al., 2023).

b) Equant: A rock block characterized by geometrically similar dimensions and commonly encountered in more circular, naturally occurring rockfall events. Due to its geometry, it has a stable and predictable trajectory (Glover et al., 2012; 2015).

c) Elongated: This rock type represents the ignimbrite blocks observed in the study area and exhibits a geometry that is almost similar to the direct toppling failure type. It is characterized by one dominant axis, with a longer dimension of approximately 1.5 m (Glover et al., 2015).

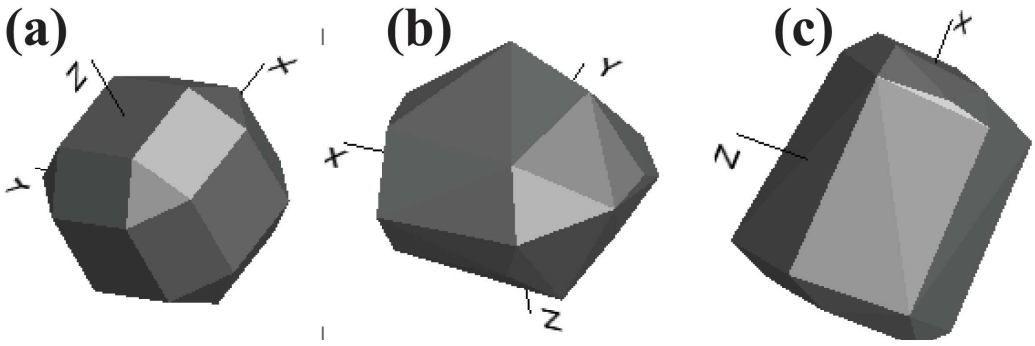

Figure 6: The rock block types used in the 3D rockfall simulations: (a) Eota, (b) Equant, and (c) Elongated.

Table 1: Geometrical and physical properties of modeled rock blocks derived from RAMMS: Rockfall software library

Rock type	Density	Dimensions (X, Y, Z)	Volume	Mass
EOTA	2700.0 kg/m^3	1.62 m x 1.62 m x 1.62 m	4.25 m^3	11475 kg
Equant	2700.0 kg/m^3	2.08 m x 1.74 m x 1.39 m	5.03 m^3	13581 kg
Elongated	2700.0 kg/m^3	2.00 m x 1.47 m x 1.34 m	3.94 m^3	10638 kg

2.5. Validation Approach: Pixel-Based and Distance-Based Methods

The validation of model results obtained at different DSM resolutions and rock block geometries was assessed by their spatial agreement with observed rockfall blocks in the field. In this context, both pixel-based and distance-based validation approaches were applied to assess model performance. Accordingly, the pixel-based validation method is defined as follows (Eq.1):

$$Accuracy_{pixel} = \frac{N_{correct}}{N_{total}} * 100 \quad (Eq\ 1).$$

$N_{correct}$: represents the total number of observed rockfall blocks

N_{total}: represents the total number of observed rockfall blocks

For this purpose, the modeled deposition outputs (number of deposited) and the point-based dataset of observed rockfall blocks, digitized from orthomosaic imagery, were used.

Within the pixel-based validation approach, the point-based observed rockfall data were spatially overlaid with the modeled deposition outputs. Each observed rock block was matched to its corresponding modeled deposition pixel, enabling the spatial relationship between model-defined deposition areas and observed rockfall occurrences to be evaluated. In the distance-based validation approach, buffer zones with distances of 1 m, 2 m, 5 m, and 10 m were generated around the modeled deposition areas. The number of observed rockfall blocks located within these buffer zones was then calculated and expressed as a proportion of the total number of observed rockfall blocks. Accordingly, the distance-based validation metric is defined as follows (Eq. 2).

$$Accuracy_{buffer} = \frac{N_d}{N_{obs}} * 100 \qquad (Eq\ 2).$$

N_d: number of observed rockfall blocks located within the buffer distance d(1, 2, 5, and 10 m)

N_{obs}: total number of observed rockfall blocks

Figure 7: Elongate rock blocks example observed in the deposition area of the study area.

3. FINDINGS

Within the scope of 3D rockfall modeling using RAMMS, key parameters describing rockfall dynamics were derived by incorporating different block geometries and DSM resolutions. These parameters include kinetic energy (kJ), rock velocity (m/s), jump height (m), and the number of deposited blocks, which indicates the locations where rock blocks come to rest. Model outputs were analyzed separately by block geometry and DSM resolution. A total of 9 modeling scenarios were conducted, combining 3 block geometries with 3 DSM resolutions. For each model, 20,000 rock blocks were simulated, resulting in a total of 180,000 modeled rock blocks. Thus, the simulations were conducted to determine the maximum probability of rock-block trajectories and behaviors during descent. The modeling process was performed using hardware equipped with a 32-core AMD Ryzen 9955HX3D processor and 64 GB DDR5 (5600 MHz) RAM.

3.1. Kinetic Energy (kJ)

The kinetic energy values obtained from the three different rock block types show clear differences. Accordingly, the highest maximum kinetic energy values across all block types and all resolution levels are observed in the EOTA block type. These values are 3925 kJ at 25 cm

resolution, 3718 kJ at 50 cm resolution, and 3203 kJ at 1 m resolution. For the Equant rock block type, the kinetic energy values are 3203 kJ at 25 cm, 3440 kJ at 50 cm, and 3488 kJ at 1 m resolution (Figure 8 (a), (b), (c)).

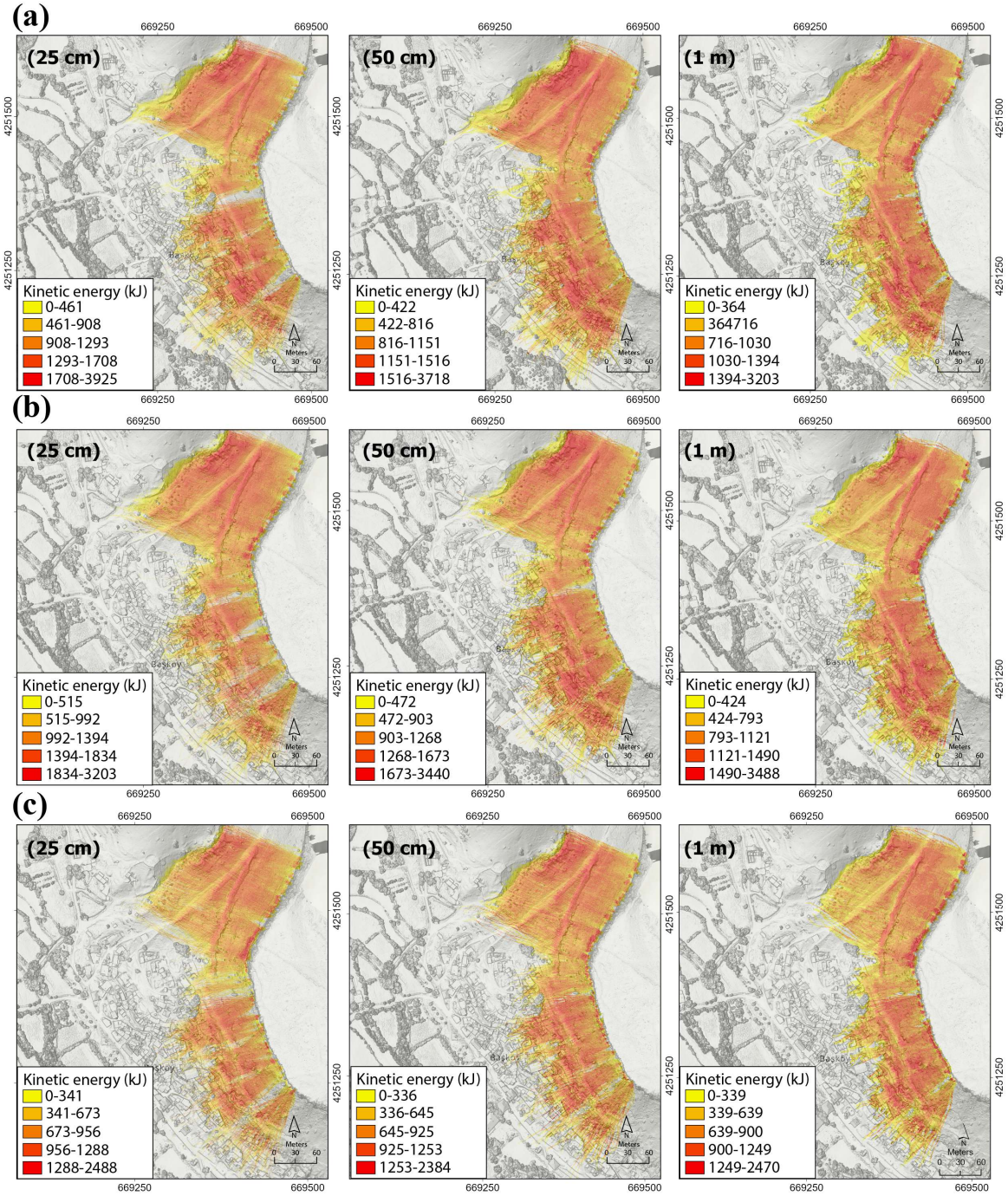

Figure 8. Spatial distribution of kinetic energy derived from rockfall simulations for different UAV-derived DSM resolutions and block geometries: (a) EOTA, (b) Equant, and (c) Elongated.

Among the three different rock block types, the elongated block type exhibits the lowest kinetic energy values. This is because the elongated block better represents the geometry of the blocks observed in the field. In addition, due to its geometry, it has a larger contact surface with the ground. The kinetic energy values for the elongated block are 2488 kJ at 25 cm, 2384 kJ at 50 cm, and 2470 kJ at 1 m resolution. Overall, the kinetic energy values across different resolutions are 722 kJ for the EOTA block type, 285 kJ for the equant block type, and 170 kJ for the elongated block type. This indicates that the EOTA block type is the most sensitive to resolution differences. The spatial distribution of kinetic energy within the study area is higher in regions with steep slopes and decreases as the slope becomes gentler. In terms of block

types, the distribution generally shows similar patterns across the area due to geometric characteristics. While the equant block type varies depending on slope changes, the energy distribution of the elongated block type is influenced by both its geometry and the geomorphological characteristics of the terrain, leading to localized concentrations in certain areas. In terms of resolution, at 25 cm resolution, the maximum energy distribution is more uniformly spread across the study area, whereas this pattern changes as the resolution decreases.

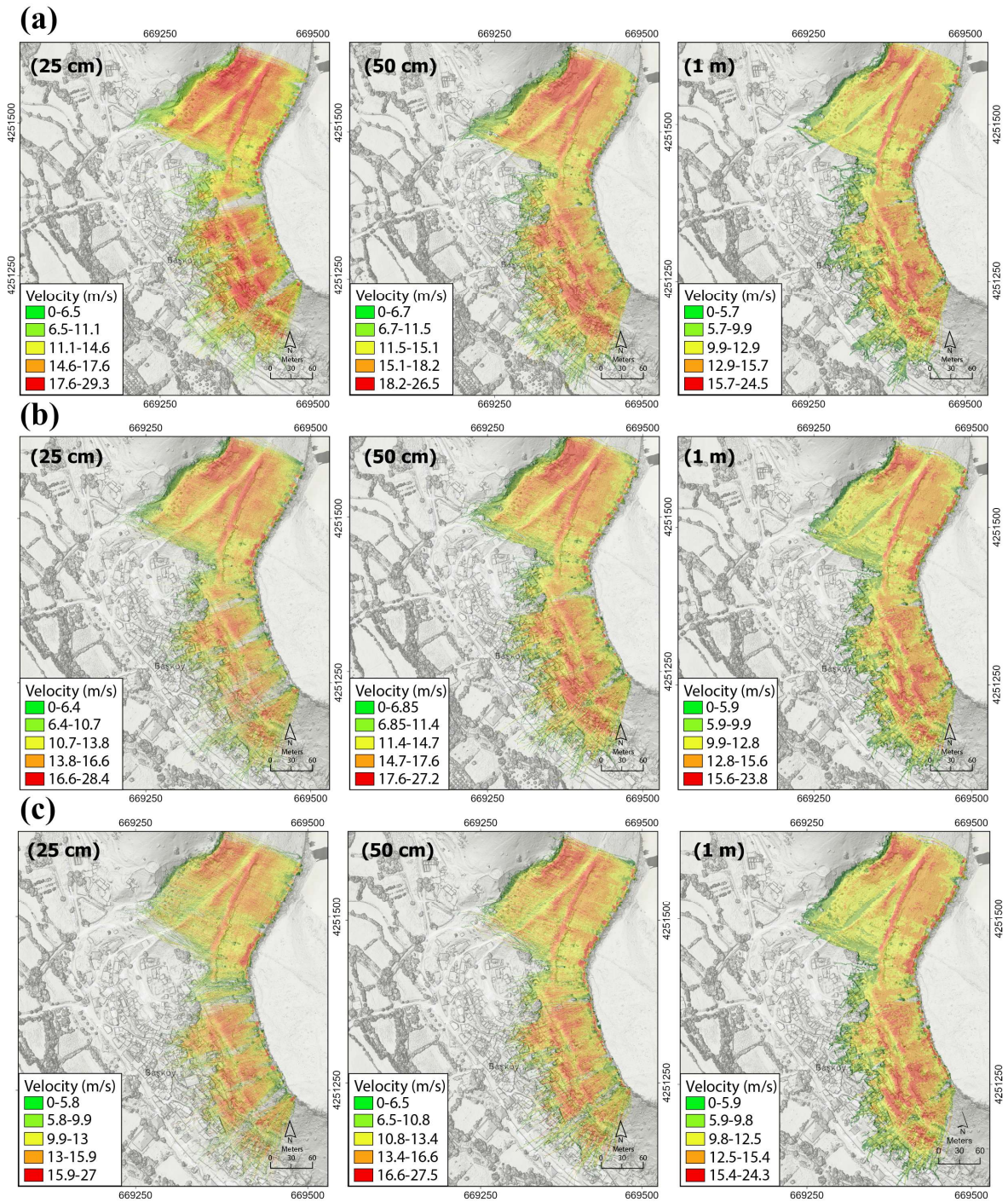

Figure 9. Spatial distribution of rockfall velocity for different UAV-derived DSM resolutions and block geometries: (a) EOTA, (b) Equant, and (c) Elongated.

3.2. Velocity (m/s)

Velocity data from rockfall modeling at different resolutions indicate that velocity varies considerably across rock block types (Figure 9 (a), (b), (c)). This pattern is similar to that observed in the kinetic energy results. Among the modeling results for the three

different rock block types at three different resolutions, the highest maximum velocity values were observed in the EOTA block type. These values were 29.3 m/s at 25 cm resolution, 26.5 m/s at 50 cm resolution, and 24.5 m/s at 1 m resolution. For the equant rock block, the corresponding values were 28.4 m/s at 25 cm resolution, 27.2 m/s at 50 cm resolution, and 23.8 m/s at 1 m resolution. For the elongated rock block, the values were 27 m/s at 25 cm resolution, 27.5 m/s at 50 cm resolution, and 24.3 m/s at 1 m resolution. In parallel with the decrease in resolution, a linear decrease in velocity values was also observed. When the maximum velocity values are evaluated, it can be seen that the EOTA block type achieved the highest velocities due to its rounded geometry, which results in limited surface contact. In contrast, the elongated rock block structure, which is more realistic and has a greater surface area, did not exhibit significant variations in velocity. Therefore, the distance and duration between the falling and damping processes of the rock blocks were relatively short. As a result, the maximum velocity values at 25 cm and 50 cm resolutions remained nearly the same, whereas a partial decrease occurred in the 1 m DSM data, where the surface became smoother, and topographic details were reduced. Based on the spatial distribution of the velocity data, rock blocks reached higher velocities on steeper slopes. In areas where the slope decreased, velocity values also decreased.

3.3. Jump height (m)

The variations observed across the nine jump-height datasets generated within the scope of the modeling are presented in Figure 10 (a), (b), (c)). Accordingly, changes in jump heights generally yielded similar values across the three rock block types and the different resolutions. However, unlike the velocity and kinetic energy variations observed in the other rock block types, the elongated rock block type exhibited different results. This situation was also clearly reflected in the jump height data. In general, kinetic energy and velocity changes decreased linearly, whereas the elongated rock block type showed an increase rather than a decrease. This variability was observed across all three different resolutions. For the elongated rock block, the maximum jump height was 22.7 m at 25 cm resolution, 22.9 m at 50 cm resolution, and 22.3 m at 1 m resolution. Generally, while the other two rock block types showed a decrease from 25 cm to 1 m resolution, the 50 cm resolution showed an increase and yielded the highest jump height values. The other jump height results generally showed an increase at resolutions of 25 cm and 50 cm, whereas the 1 m resolution showed a decreasing trend and the minimum jump height values. These results for the EOTA rock block were 24.2 m at 25 cm resolution, 25.6 m at 50 cm resolution, and 22.5 m at 1 m resolution. For the equant rock block, the values were 22.5 m at 25 cm resolution, 28.7 m at 50 cm resolution, and 21.9 m at 1 m resolution. The highest jump height values were observed in the equant rock block at 50 cm resolution, reaching 28.7 m. This can be explained by the more stable falling, progression, and damping characteristics of the equant rock block, which also help preserve energy during movement and reach maximum values. In addition, while the increased surface roughness at 25 cm resolution yielded the highest maximum velocity and kinetic energy values, the jump height data showed the highest values at 50 cm resolution. More detailed and rougher surfaces acted as barriers, leading to lower jump heights at 25 cm resolution. On the other hand, the simplified topographic detail in the 1 m DSM reduced maximum jump height values. The results from the 50 cm DSM data indicate that this resolution provides optimal conditions, as surface details are better preserved at this scale.

3.4. Spatial Distribution of Rockfall Activity

The spatial distribution of rock blocks with different geometries was compared with the damping areas obtained from the *Nr of deposited* data produced through 3D modeling at different resolutions (Figure 11 (a), (b), (c)). For this purpose, deposition density maps were generated as heatmaps using the *'Number of deposited data points' metric*. The spatial distribution of fallen blocks derived from orthomosaic data was overlaid to analyze relative density distributions. Thus, the spatial relationship between the modeled and observed rock blocks was evaluated. Fallen blocks generally show a clear concentration in the upper sections of the slopes. This situation directly reflects the failure mechanism of the fallen blocks and indicates that the rockfall

dynamics are consistent with a toppling-type failure mechanism. Models with 50 cm resolution generally produced more continuous and spatially consistent density distributions. Particularly in the equant and elongated block geometries, a stronger agreement was observed between the model results and the distribution of the observed rock blocks.

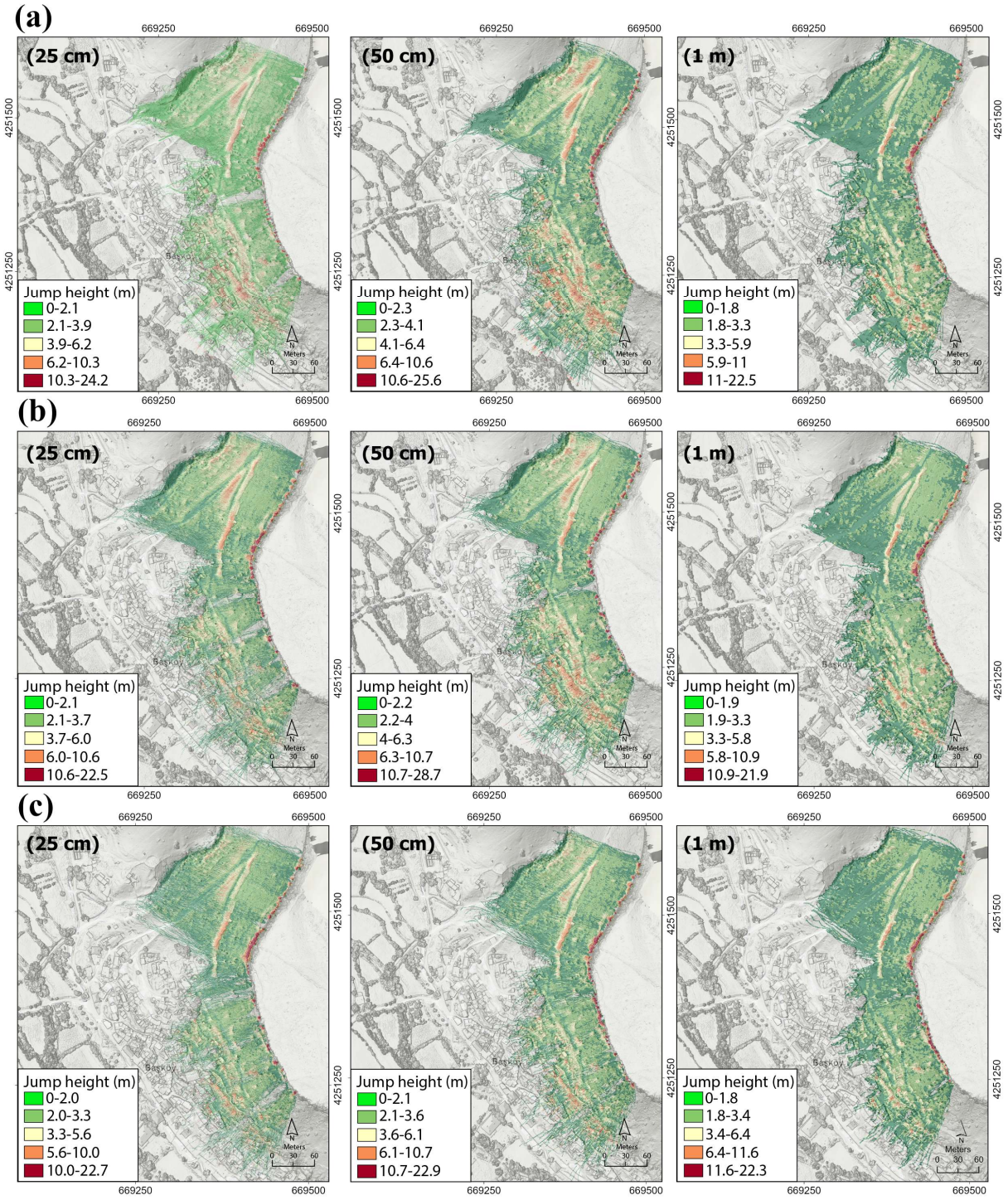

Figure 10: Spatial distribution of jump height derived from rockfall simulations for different UAV-derived DSM resolutions and block geometries: (a) EOTA, (b) Equant, and (c) Elongated.

Rock blocks exhibited a more irregular distribution and dispersed concentration patterns at the 25 cm resolution. In contrast, the 1 m resolution showed a more generalized spatial distribution. This is because decreasing resolution progressively simplifies topographic details. The distribution patterns observed according to block geometries generally followed the slope morphology. Naturally, this behavior varied depending on the geometry of the rock blocks themselves. The equant block type displayed a wider spatial distribution,

whereas the EOTA block type tended to concentrate within specific zones, particularly in areas with minimum slope where the blocks were decelerated and deposited. In the elongated block type, the geometry of the rock blocks limited their travel distance, preventing them from propagating further downslope. When all distribution patterns are evaluated together, nearly the entire study area appears to have been affected by rockfall processes. This distinction becomes more evident in the results obtained from different DSM resolutions.

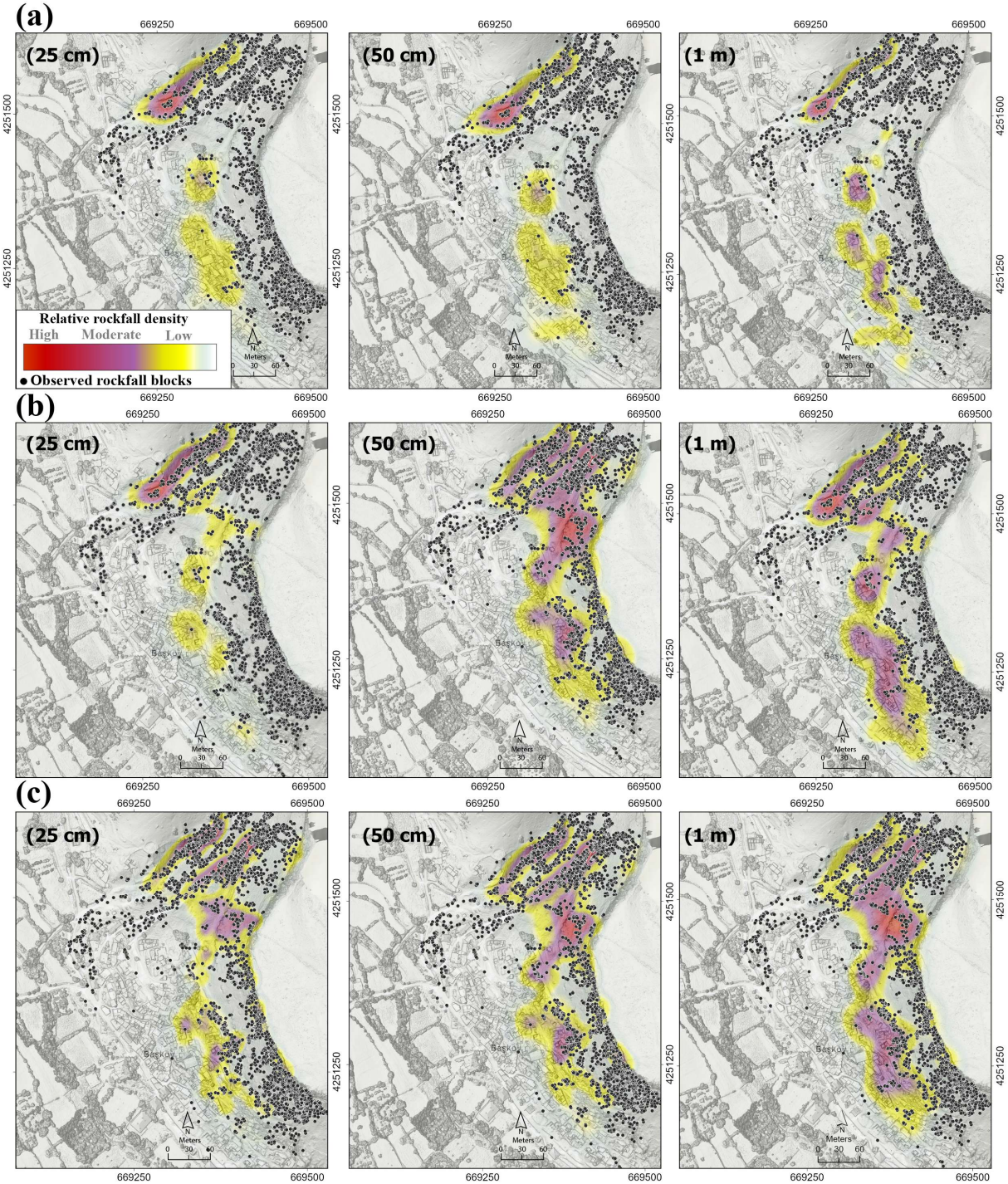

Figure 11. Relative rockfall density and spatial distribution of observed rockfall blocks for different DSM resolutions and block geometries.

3.5. Validation of the results based on Nr of Deposited rocks

The accuracy of the nine models obtained in this study was assessed by comparing them with the rock blocks observed in the field. Within this scope, fallen rock blocks were manually digitized from high-resolution orthomosaic data, yielding a total of 4,299 rock

blocks. Thus, the spatial relationship between the observed and modeled rock blocks was evaluated using both pixel-based and distance-based validation approaches. The pixel-based validation analyses yielded unrealistic results for the models due to positional mismatches between the observed and modeled rock blocks. This is because the pixels representing the locations where the modeled rock blocks fell did not spatially overlap with the pixels representing the fallen rock blocks, even at very short distances. In this case, the modeled rock blocks did not fall exactly on the pixels where the rock blocks were actually located. Therefore, distance-based validation was preferred. According to the distance-based validation results, model accuracy varied directly with DSM resolution and block shape. The highest spatial agreement was observed at 50 cm resolution with the elongated rock block type, where the highest success rates were achieved at the 5 m and 10 m distance thresholds (Figure 12 (a), (b), (c)). The elongated rock type also represents the most realistic rock block geometry observed in the field. On the other hand, although the 25 cm resolution reflected the highest level of detail and surface features in the DSM data, it did not produce the best results. This can be explained by the fact that the highly detailed topographic representation increased the sensitivity to the complex nature of rockfall processes during block movement.

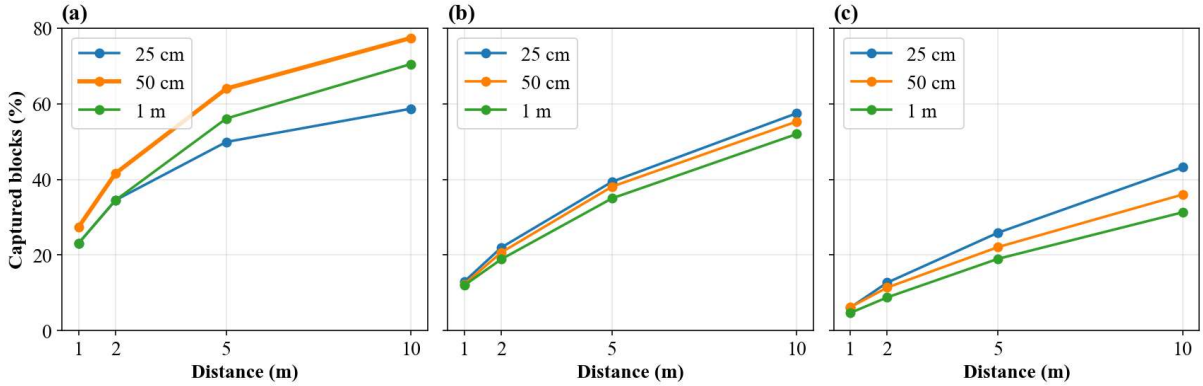

Figure 12: Distance-based validation of both observed and modeled rock blocks (a) Elongated, (b) Equant, and (c) EOTA

4. DISCUSSION

Determining the optimal resolution of UAV-derived DSM data for rockfall modeling is critical for both data production and model performance. Producing data at different resolutions involves significant differences in planning, time requirements, equipment capacity, and data processing workflows. In particular, generating a high-resolution DSM dataset requires considerably more time and also demands an appropriate computational infrastructure for processing. Therefore, instead of simply preferring the highest resolution available, it is necessary to maintain a proper balance between model accuracy and data production cost. According to this study's modeling results, the effect of DSM resolution on rockfall dynamics depends on the model's surface representation. Velocity values reached their highest levels in the EOTA block geometry, which is particularly preferred for barrier and protective measure design, using 25 cm-resolution DSM data. This indicates that topographic relief characteristics are well preserved at the 25 cm resolution. However, this situation must also be explained by the geometric properties of the rock block type itself. During rock block movement, the friction coefficient at the surface plays a major role. This effect is clearly observed in the elongated and equant block types. While surface roughness is well preserved at high resolution, the rock block's response to it is equally important.

When the influence of block type on the model results is evaluated, elongated blocks yield more realistic results. This is because they produced more linear, continuous trajectories, resulting in greater agreement between the observed fallen rock blocks and the modeled

blocks. This agreement remained lower in the other rock block types. In contrast, at the 1 m resolution, where surface roughness decreases, the simplification of surface details is directly reflected in the model outputs. At the 50 cm resolution, however, a balance exists between surface roughness representation and model generalization, allowing rockfall dynamics to be represented more realistically and effectively. It was also observed that there is no direct linear relationship between velocity, kinetic energy, and bounce height. The datasets with the highest kinetic energy did not necessarily correspond to the highest bounce heights. This result reflects the multi-parameter and complex nature of rockfall processes. Considering the validation results, pixel-based validation tends to underestimate model performance because it is highly sensitive to small positional deviations in models with narrow, linear rockfall trajectories. In contrast, the distance-based analysis approach allows the rebound and dispersion processes of rock blocks to be evaluated more realistically in spatial terms, thereby improving validation accuracy.

5. CONCLUSION

This study focuses on the realistic modeling of rockfall potential in the Başköy settlement area, where active rockfall events frequently occur, and comprehensively evaluates the effects of different DSM resolutions and rock block geometries on 3D rockfall modeling results. The findings demonstrate that under the same terrain conditions, high-resolution DSM data alone are insufficient for rockfall studies, and that topographic characteristics must also be considered. In this context, determining the optimal resolution is critically important for improving model accuracy and guiding future studies. The modeling results revealed that maximum velocity and kinetic energy values were more pronounced in high-resolution DSM datasets, whereas spatial distribution patterns and bounce behavior produced more balanced results at medium resolution (50 cm). This indicates that the 50 cm resolution provides an optimal balance between topographic detail and model generalization. When the effect of block geometry was evaluated, the EOTA block type produced higher velocity and energy values, while the elongated block type exhibited more linear, continuous movement behavior and achieved the best agreement with the observed field distribution. The equant block geometry displayed a more balanced behavior between these two extremes. Validation results showed that model performance is sensitive to both DSM resolution and block geometry, with the highest spatial agreement obtained in the elongated block scenario at 50 cm resolution. In addition, the pixel-based validation approach was found to underestimate model performance.

In conclusion, this study demonstrates that approaches based on a single block geometry are insufficient for rockfall modeling and that different block types should be evaluated together. The findings indicate that considering resolution and block geometry simultaneously is critical for improving model accuracy and provides an important methodological framework for future studies.

ACKNOWLEDGEMENTS

This study was supported by the Scientific and Technological Research Council of Türkiye (TUBITAK) under Grant Number 125Y054. The authors thank TUBITAK for their support

REFERENCES

Abellán, A., Vilaplana, J. M., & Martínez, J. (2006). Application of a long-range Terrestrial Laser Scanner to a detailed rockfall study at Vall de Núria (Eastern Pyrenees, Spain). *Engineering geology*, *88*(3-4), 136-148.

AFAD. (2021). T.C. Kayseri Valiliği, İl Afet ve Acil Durum Müdürlüğü, İl Afet Risk Azaltma Planı, Kayseri. 151p.

Akın, M., Dinçer, İ., Ok, A. Ö., Orhan, A., Akin, M. K., & Topal, T. (2021). Assessment of the effectiveness of a rockfall ditch through 3-D probabilistic rockfall simulations and automated image processing. *Engineering Geology*, *283*, 106001.

Alvioli, M., Santangelo, M., Fiorucci, F., Cardinali, M., Marchesini, I., Reichenbach, P., ... & Peruccacci, S. (2021). Rockfall susceptibility and network-ranked susceptibility along the Italian railway. *Engineering Geology*, *293*, 106301.

Alvioli, M., Falcone, G., Mendicelli, A., Mori, F.,

Fiorucci, F., Ardizzone, F., & Moscatelli, M. (2023). Seismically induced rockfall hazard from a physically based model and ground motion scenarios in Italy. *Geomorphology*, *429*, 108652.

Arsenith, L. J. (2025). *Influence of Terrain Model Resolution on Rockfall Dispersion and Tortuosity of Rockfall Paths*. Boise State University. Master of Science in Civil Engineering Boise State University.

Atabey, E. 1989. *"1/100.000 Ölçekli Açınsama Nitelikli Türkiye Jeoloji Haritaları Serisi: Kayseri L33 Paftası"*. Maden Tetkik ve Arama Genel Müdürlüğü, Ankara .

Bartelt, P., Gerber, W., Christen, M., & Bühler, Y. (2016). Modeling rockfall trajectories with non-smooth contact/impact mechanics [Modeling rockfall trajectories with non-smooth contact/impact mechanics]. In 13th Congress Interpraevent 2016 (pp. 203–211). Lucerne, Switzerland.

Bolliger, D., Schlunegger, F., and McArdell, B. W. (2024). Comparison of debris flow observations, including fine-sediment grain size and composition and runout model results, at Illgraben, Swiss Alps, Nat. Hazards Earth Syst. Sci., 24, 1035–1049, https://doi.org/10.5194/nhess-24-1035-2024.

Bühler, Y., Christen, M., Glover, J., Christen, M., & Bartelt, P. (2016). Significance of digital elevation model resolution for numerical rockfall simulations Significance of digital elevation model resolution.... In 3rd RSS Rock Slope Stability Conference (pp. 1-8). Lyon, France.

Carlà, T., Nolesini, T., Solari, L., Rivolta, C., Dei Cas, L., and Casagli, N. (2019). Rockfall forecasting and risk management along a major transportation corridor in the Alps through ground-based radar interferometry, Landslides, 16, 1425–1435, https://doi.org/10.1007/s10346-019-01190-y.

Caviezel, A., Demmel, T., Ringenbach, A., & Bühler, Y. (2019). RAMMS::ROCKFALL: A novel 3D contact algorithm for rockfall simulations RAMMS::ROCKFALL: A novel 3D contact algorithm.... Proceedings of the 53rd US Rock Mechanics/Geomechanics Symposium, ARMA 19-223.

Caviezel, A., Ringenbach, A., Demmel, S. E., Dinneen, C. E., Krebs, N., Bühler, Y., Christen, M., Meyrat, G., Stoffel, A., Hafner, E., Eberhard, L. A., Rickenbach, D. von, Simmler, K., Mayer, P., Niklaus, P. S., Birchler, T., Aebi, T., Cavigelli, L., Schaffner, M., Rickli, S., Schnetzler, C., Magno, M., Benini, L., and Bartelt, P. (2021) The relevance of rock shape over massimplications for rockfall hazard assessments, Nature Communications, 12, 5546, https://doi.org/10.1038/s41467-021-25794-y,

Chatziangelis, E., Michalopoulou, M., Depountis, N., Pelekis, P., & Agrevi, M. (2025). Three-Dimensional Stability of Rocky Slopes and Identification of Hazard Zones in Monuments of Archaeological Interest: Case Study of Ancient Corinth, Greece. *Geosciences*, *15*(6), 199.

Christen, M., Bühler, Y., Glover, J., Gerber, W., & Bartelt, P. (2014). *Ramms::Rockfall*. *1*(April 2012).

Corominas, J., van Westen, C., Frattini, P., Cascini, L., Malet, J. P., Fotopoulou, S., Catani, F., Van Den Eeckhaut, M., Mavrouli, O., Agliardi, F., Pitilakis, K., Winter, M. G., Pastor, M., Ferlisi, S., Tofani, V., Hervás, J., & Smith, J. T. (2014). Recommendations for the quantitative analysis of landslide risk. *Bulletin of Engineering Geology and the Environment*, *73*(2), 209–263. https://doi.org/10.1007/s10064-013-0538-8

Crosta, G. B., Agliardi, F., Frattini, P., & Lari, S. (2015). Key Issues in Rock Fall Modeling, Hazard and Risk Assessment for Rockfall Protection Key Issues in Rock Fall Modeling.... In G. Lollino et al. (Eds.), Engineering Geology for Society and Territory—Volume 2 (pp. 43–48). Springer, Cham Springer Link.

Dorren, L., & Kühne, R. (2016). Comparing the 3D rockfall simulation models Rockyfor3D and RAMMS :: ROCKFALL at a case study site in Switzerland. In *INTERPRAEVENT 2016 – Extended Abstracts* (pp. 2–3).

Erol, O. (1983). "Türkiye'nin genç tektonik ve jeomorfolojik gelişimi". Jeomorfoloji Dergisi, (11), 1-22.

Glover, J., Bartelt, P., Christen, M., & Gerber, W.

(2015). Rockfall-Simulation with Irregular Rock Blocks. In *Engineering Geology for Society and Territory - Volume 2: Landslide Processes* (Vol. 2, pp. 1–2177). https://doi.org/10.1007/978-3-319-09057-3

Glover, J., Denk, M., Bourrier, F., Volkwein, A., & Gerber, W. (2012). Measuring the kinetic energy dissipation effects of rockfall attenuating systems using video analysis. *Proc. Interpraevent Congress*, *1*, 151–160.

Gallo, I. G., Martínez-Corbella, M., Sarro, R., Iovine, G., López Vinielles, J., Hérnandez, M., Robustelli, G., Mateos, R. M., and García-Davalillo, J. C. (2021). An Integration of UAV-Based Photogrammetry and 3D Modelling for Rockfall Hazard Assessment: The Cárcavos Case in 2018 (Spain), Remote Sensing, 13, 3450, https://doi.org/10.3390/rs13173450.

Guzzetti, F., Reichenbach, P., Ghigi, S., (2004). Rockfall hazard and risk assessment along a transportation corridor in the Nera Valley, Central Italy. Environ. Manag. 34 (2), 191–208. https://doi.org/10.1007/s00267-003-0021-6s

Hungr, O., Leroueil, S., & Picarelli, L. (2014). The Varnes classification of landslide types, an update. *Landslides*, *11*(2), 167–194. https://doi.org/10.1007/s10346-013-0436-y

Jaboyedoff, M., Oppikofer, T., Abellán, A., Derron, M. H., Loye, A., Metzger, R., & Pedrazzini, A. (2012). Use of LIDAR in landslide investigations: a review. *Natural hazards*, *61*(1), 5-28.

Jacobs, B., Ismael, M., Ezzy, M., Keuschnig, M., Mendler, A., Kieser, J., ... & Helal, H. (2026). Safeguarding Cultural Heritage: Integrating laser scanning, InSAR, vibration monitoring and rockfall/granular flow runout modelling at the Temple of Hatshepsut, Egypt. *Earth Surface Dynamics*, *14*(1), 55-74.

Kakavas, M., & Nikolakopoulos, K. G. (2022). The influence of DSM on rock-fall simulation: a case study from Western Greece. In K. Schulz, K. G. Nikolakopoulos, & U. Michel (Eds.), *Earth Resources and Environmental Remote Sensing/GIS Applications XIII* (p. 44). SPIE. https://doi.org/10.1117/12.2636139

Lan, Hengxing, C. Derek Martin, Chenghu Zhou, & Chang Ho Lim. (2010). "Rockfall hazard analysis using LiDAR and spatial modeling." *Geomorphology* 118, no. 1-2, 213-223.

Lanfranconi, C., Frattini, P., Sala, G., Dattola, G., Bertolo, D., Sun, J., & Crosta, G. B. (2023). Accounting for the effect of forest and fragmentation in probabilistic rockfall hazard. *Natural Hazards and Earth System Sciences*, *23*(6), 2349–2363. https://doi.org/10.5194/nhess-23-2349-2023

Loye, A., Jaboyedoff, M., Pedrazzini, A. (2009). Identification of potential rockfall source areas at a regional scale using a DEM-based geomorphometric analysis. Nat. Hazards Earth Syst. Sci. 9, 1643–1653. https://doi.org/10.5194/nhess-9-1643-2009.

Mary Vick, L., Zimmer, V., White, C., Massey, C., & Davies, T. (2019). Significance of substrate soil moisture content for rockfall hazard assessment. *Natural Hazards and Earth System Sciences*, *19*(5), 1105–1117. https://doi.org/10.5194/nhess-19-1105-2019

Massaro, L., Forte, G., De Falco, M., Rauseo, F., & Santo, A. (2024). Rockfall source identification and trajectory analysis from UAV-based data in volcano-tectonic areas: a case study from Ischia Island, Southern Italy. *Bulletin of Engineering Geology and the Environment*, *83*(3), 1–17. https://doi.org/10.1007/s10064-024-03569-1

Mavrouli, O., Corominas, J., & Jaboyedoff, M. (2015). Size Distribution for Potentially Unstable Rock Masses and In Situ Rock Blocks Using LIDAR-Generated Digital Elevation Models. *Rock Mechanics and Rock Engineering*, *48*(4), 1589–1604. https://doi.org/10.1007/s00603-014-0647-0

Milan, L., Napoli, M. L., Barbero, M., & Castelli, M. (2023). A Novel Approach to Assess the Influence of Rockfall Source Areas: The Case Study of Bardonecchia (Italy). *Geosciences*, *13*(12), 386. https://doi.org/10.3390/geosciences13120386

Öztürk, M. Z., Utlu, M., & Şimşek, M. (2022). UAV-based 3D modeling analysis in determining and preventing rockfall hazard: A case study from Murtaza Village (Niğde, Turkey). *Yerbilimleri/Earth Sciences*, *43*(2),

182–196. https://doi.org/10.17824/yerbilimleri.1021032

Pasquarè, G., Poli, S., Vezzoli, L. & Zanchi, A. (1988). Continental arc volcanism and tectonic setting in Central Anatolia, Turkey, Tectonophysic, 146, 217-230

Ringenbach, A., Bebi, P., Bartelt, P., Rigling, A., Christen, M., Bühler, Y., Stoffel, A., & Caviezel, A. (2023). Shape still matters: rockfall interactions with trees and deadwood in a mountain forest uncover a new facet of rock shape dependency. *Earth Surface Dynamics*, *11*(4), 779–801. https://doi.org/10.5194/esurf-11-779-2023

Sarkar, N., Devoto, S., Vandelli, V., Rossi, S., Soldati, M., & Rizzo, A. (2024). Rock-fall runout simulation using a QGIS plugin along north–west coast of Malta (Mediterranean Sea). *Natural Hazards*, *120*(15), 14553-14570.

Sarro, R., Rossi, M., Reichenbach, P., & Mateos, R. M. (2025). From rockfall source area identification to susceptibility zonation: a proposed workflow tested on El Hierro (Canary Islands, Spain). *Natural Hazards and Earth System Sciences*, *25*(4), 1459-1479.

Schraml, K., Thomschitz, B., McArdell, B. W., Graf, C., and Kaitna, R. (2015). Modeling debris-flow runout patterns on two alpine fans with different dynamic simulation models, Nat. Hazards Earth Syst. Sci., 15, 1483–1492, https://doi.org/10.5194/nhess-15-1483-2015.

Somuncu, M. (1988). "Develi Ovası'nın Kuzey ve Batı Bölümünde Rüzgâr Erozyonu Sorunu ile Alınması Gereken Önlemler Üzerine Bir Araştırma", Yayımlanmamış Yüksek Lisans Tezi, Ankara Üniversitesi Sosyal Bilimler Enstitüsü, Ankara.

Sür, Ö. (1972). Türkiye'nin Özellikle İç Anadolu'nun Genç Volkanik Alanlarının Jeomorfolojisi Ankara Üniversitesi Dil ve Tarih-Coğrafya Fakültesi Yayınları, Ankara, s.120.

Torsello, G., Vallero, G., & Castelli, M. (2021). The role of block shape and slenderness in the preliminary estimation of rockfall propagation. *IOP Conference Series: Earth and Environmental Science*, *833*(1), 012177. https://doi.org/10.1088/1755-1315/833/1/012177

Ulamış, K. (2026). Evaluation of protective measures against rockfall hazard with 3D analysis: Mardin Castle, Türkiye. Environmental Earth Sciences, 85, Makale no: 476. Springer - Environmental Earth Sciences

Utlu, M., Öztürk, M. Z., & Şimşek, M. (2020b). Rockfall analysis based on UAV technology in Kazıklıali Gorge, Aladağlar (Taurus Mountains, Turkey). *International Journal of Environment and Geoinformatics*, *7*(3), 239–251. https://doi.org/10.30897/ijegeo

Utlu, M., Öztürk, M. Z., & Şimşek, M. (2020a). Emli Vadisi'ndeki (Aladağlar) Talus Depolarının Kantitatif Analizlere Göre İncelenmesi. In S. Birinci, Ç. Kıvanç Kaymaz, & Y. Kızılkan (Eds.), *Coğrafi Perspektifle Dağ ve Dağlık Alanlar (Sürdürülebilirlik-Yönetim-Örnek Alan İncelemeleri)* (I., pp. 51–72). Kriter Yayınevi.

Utlu, M., Öztürk, M. Z., & Şimşek, M. (2021). Yüksek Çözünürlüklü Sayısal Yüzey Modellerine Uygulanan Üç Boyutlu Analizler ile Kaya Düşmelerine Ait Sayısal Risk Değerlendirmesi: Ünlüyaka Köyü (Niğde, Türkiye). In M. F. Döker & E. Akköprü (Eds.), *Coğrafya Araştırmalarında Coğrafi Bilgi Sistemleri Uygulamaları II* (I., pp. 51–69). Pegem Akademi. https://doi.org/10.14527/9786257676489

Utlu, M., Öztürk, M. Z., Şimşek, M., & Akgümüş, M. F. (2023). Evaluation of rockfall hazard based on UAV technology and 3D Rockfall Simulations. *International Journal of Environment and Geoinformatics*, *10*(4), 1–16. https://doi.org/10.30897/ijegeo.1323768

Utlu, M., & Şimşek, M. (2025). Yüksek Dağlık Alanlarda Kaya Düşme Çalışmalarında Farklı Çözünürlükte Sayısal Yüzey Modeli (SYM) Verilerinin Kullanım. In İ. Çiçek, E. Öner, & R. İlhan (Eds.), *Prof. Dr. Erdoğan AKKAN Anısına FİZİKİ COĞRAFYA ARAŞTIRMALARI* (Birinci Ba, pp. 489–496). Ege Üniversitesi Yayınları.

Vagionakis, N., Diamantis, K., Andreadakis, E., & Stavropoulou, M. (2026). UAV based photogrammetry and rockfall hazard assessment at the Vrachon Theatre in Greece. Geotechnical and Geological Engineering, 44(1), 71-85.

Varnes, D.J. (1978). Slope movement types and processes. In *Landslide Analysis and Control*; Special Report 176; Schuster, R.L., Krizek, R.J., Eds.; National Academy of Sciences: Washington, DC, USA, pp. 11–33.

Vo, D. T. (2015). *RAMMS :: Rockfall versus Rockyfor3D in rockfall trajectory simulations at the Community of Vik , Norway Dam Thanh Vo RAMMS :: Rockfall versus Rockyfor3D in rockfall trajectory simulations at the Community of Vik , Norway*. University of Oslo, Faculty of Mathematics and Natural Sciences, Master Thesis in Geosciences.

Volkwein, A., Schellenberg, K., Labiouse, V., Agliardi, F., Berger, F., Bourrier, F., Dorren, L. K. A., Gerber, W., & Jaboyedoff, M. (2011). Rockfall characterisation and structural protection – a review. *Natural Hazards and Earth System Sciences*, *11*(9), 2617–2651. https://doi.org/10.5194/nhess-11-2617-2011.

Wendeler, C., Bühler, Y., Bartelt, P., and Glover, J. (2017). Application of three-dimensional rockfall modelling to rock face engineering, Geomechanics and Tunnelling, 10, 74–80, https://doi.org/10.1002/geot.201600073.

Žabota, B., Repe, B., & Kobal, M. (2019). Influence of digital elevation model resolution on rockfall modelling. *Geomorphology*, *328*, 183-195.

Zengin, Ü. B., & Ulamış, K. (2025). Üç Boyutlu Kaya Düşmesi Analizlerinde Blok Geometrisi Etkisinin İncelenmesi (Gölbaşı, Ankara). *Jeoloji Mühendisliği Dergisi*, *49*(2), 3-22. https://doi.org/10.24232/jmd.1728155